



ISSN: 2617-6548

URL: [www.ijirss.com](http://www.ijirss.com)

## Design electrical model noise and perform nonlinearities of SiGe bipolar phototransistor

 Ahmadou Moustapha Diop<sup>1\*</sup>,  Jean-Luc Polleux<sup>2</sup>,  Catherine Algani<sup>3</sup>,  Said Mazer<sup>4</sup>,  Mohammed Fattah<sup>5</sup>,  
 Moulhime EL Bekkali<sup>6</sup>

<sup>1,4,6</sup>*IASSE Laboratory, University Sidi Mohamed Ben Abdellah Fez, Morocco.*

<sup>2</sup>*University Paris-Est, ESYCOM (EA 2552), ESIEE, UPEM, Le Cnam, Noisy-le-Grand, France.*

<sup>3</sup>*Le Cnam, ESYCOM (EA2552), Paris, France.*

<sup>5</sup>*IMAGE Laboratory, Moulay Ismail University, Meknes, Morocco.*

Corresponding author: Ahmadou Moustapha Diop (Email: [diopmbaomoustapha@yahoo.fr](mailto:diopmbaomoustapha@yahoo.fr))

### Abstract

This study uses a new model developed in this paper to investigate the performance of a heterojunction phototransistor (HPT) on SiGe technology. An electrical model of an optical window phototransistor was developed based on the Ebers & Moll model, and its performance was evaluated by examining the error vector magnitude (EVM) when integrated into a mobile communication setup. Simulations showed that the HPT exhibited an EVM lower than 8%, enabling 64-Quadrature Amplitude Modulation (64-QAM) modulation for the mobile network. The third-order intercept point (IP3) measured 22 dBm, making the HPT suitable for Radio over Fiber (RoF) links in the detection block. The noise model of the HPT was also studied, resulting in a favorable power spectral density (PSD) that facilitates accurate modeling and prediction of the noise behavior of HPTs across various applications. This study provides valuable insights into the performance of HPTs on SiGe technology, enabling the development of more precise and efficient models for future research and practical applications. The results carry significant implications for the use of HPTs in optical communication systems.

**Keywords:** Error vector magnitude, Heterojunction phototransistor, Noises, The third-order intercept point (IP3).

**DOI:** 10.53894/ijirss.v6i4.1896

**Funding:** This study received no specific financial support.

**History: Received:** 30 March 2023/**Revised:** 10 May 2023/**Accepted:** 23 June 2023/**Published:** 17 July 2023

**Copyright:** © 2023 by the authors. This article is an open access article distributed under the terms and conditions of the Creative Commons Attribution (CC BY) license (<https://creativecommons.org/licenses/by/4.0/>).

**Authors' Contributions:** All authors contributed equally to the conception and design of the study. All authors have read and agreed to the published version of the manuscript.

**Competing Interests:** The authors declare that they have no competing interests.

**Transparency:** The authors confirm that the manuscript is an honest, accurate, and transparent account of the study; that no vital features of the study have been omitted; and that any discrepancies from the study as planned have been explained.

**Institutional Review Board Statement:** The Ethical Committee of the University Sidi Mohammed Ben Abdellah, Morocco has granted approval for this study.

**Data Availability Statement:** The corresponding author may provide study data upon reasonable request.

**Publisher:** Innovative Research Publishing

### 1. Introduction

Recently, there has been a growing interest in SiGe/Si heterojunction bipolar phototransistors (HPTs) as an attractive alternative for high-speed optical communication systems. These devices have been extensively studied for various applications, including optocouplers, optical switches, and optical receivers. With the increasing demand for high-speed communication systems, such as 5G and 6G networks, the development of SiGe/Si HPT devices has become more significant.

Their potential to improve the performance of optical communication systems has led to their increased exploration and utilization [1].

The nonlinear behavior of SiGe/Si HPT devices has been a significant concern regarding their use in high-speed optical receivers, as it can potentially affect their accuracy. To address this issue, researchers have focused on increasing the error vector magnitude (EVM) of these devices [2, 3]. In the construction of high-speed optical communication systems, the third-order intercept point (IP3) of SiGe/Si HPT devices holds a critical consideration [4]. Optimizing the IP3 of these devices can greatly enhance their performance in such systems. Researchers have employed various techniques such as pre-distortion [5], digital signal processing [6], and IP3 tuning, to achieve this. These methods have demonstrated effectiveness in improving the performance of SiGe/Si HPT devices.

Characterization of noise in SiGe/Si HPT devices is another crucial area of research [7]. Noise can have adverse effects on high-speed optical communication systems, and understanding the noise response of SiGe/Si HPT devices can help develop more reliable and robust systems. Numerous studies have focused on analyzing and reducing the noise performance of SiGe/Si HPT devices [2]. Moreover, methods for noise cancellation and suppression [8, 9] have been developed. The high-frequency response of SiGe/Si HPT devices has also been a research subject, with techniques such as device optimization [3] and impedance matching [10] being used to improve their performance.

SiGe/Si HPT devices have gained attention for their potential applications in sensing [11] and imaging [12], along with high-speed optical communication systems. These devices exhibit fast response times and low noise performance, making them suitable for detecting and amplifying weak signals in these applications. The advancement in fabrication technology has also influenced the development of SiGe/Si HPT devices. Researchers have explored modern techniques such as molecular beam epitaxy (MBE) [13] and metal-organic chemical vapor deposition (MOCVD) to improve the performance of these devices. Furthermore, GaAs and InP have also been studied as potential alternative materials for SiGe/Si HPT devices [14, 15].

The importance of SiGe/Si HPT devices in high-speed communication systems, including 5G and 6G networks, is increasing due to their excellent noise performance and temporal response [16]. In addition to their use in optical communication systems, SiGe/Si HPT devices are also suitable for radio-over-fiber (RoF) systems [17]. RoF systems offer a compelling alternative for various applications as they combine the bandwidth of optical fibers with the mobility of wireless communication [18]. Therefore, the potential of SiGe/Si HPT devices in RoF systems offers significant advantages for the development of advanced communication systems.

SiGe/Si HPT devices play a critical role in enabling high-speed data transfer and communication across various applications. These devices have been extensively researched for high-speed optical communication systems, radio-over-fiber (RoF) systems, and other applications like healthcare and manufacturing [19]. The quick response times and low noise performance of SiGe/Si HPT devices make them well-suited for these applications, ensuring the efficient operation of systems and processes [20]. Therefore, further research on SiGe/Si HPT devices is essential for developing high-speed communication systems and applications. These advantages make SiGe/Si HPT devices highly suitable for high-speed data transmission applications [21].

This article builds upon previous studies on the HPTs, which aimed to establish a viable electrical model based on Ebers & Moll components [22]. Based on the obtained results for static and dynamic parameters, we will define a building model in Advanced Design System (ADS) that meets the requirements outlined in the literature for SiGe/Si phototransistors. In addition to completing the electrical model, we have also studied nonlinearities, focusing on EVM for a Long-Term Evolution (4G LTE) communication system. The choice of the 4G network is motivated by the measurements taken on the SiGe/Si HPT to validate the electrical model. This research aims to contribute to developing more efficient and effective phototransistors for use in modern communication systems.

Ongoing research has provided valuable insights into the behavior and performance of SiGe/Si HPT devices and methods for enhancing their performance across different applications. With the increasing demand for high-speed communication systems, the importance of SiGe/Si HPT devices is expected to grow, making them a crucial area of research for the future.

## **2. Structure and Properties of HPT 10SQxEBC SiGe/Se**

The SiGe/Si heterojunction bipolar phototransistor (HPT) is a promising component for high-speed optical communication systems due to its good characterization, quick temporal response, and noise performance [23]. SiGe/Si HPT devices are perfect for high-speed optical receivers as they can efficiently detect and amplify weak optical signals. In addition to high-speed optical receivers, SiGe/Si HPT devices have been investigated for use in high-speed optocouplers and optical switches.

This work utilizes the Telefunken GmbH 80-GHz SiGe Bipolar process technology to create the HPT [24]. This technology allows for developing circuits operating over 10 GHz and up to 60 GHz in certain combinations [25]. The HPT can be manufactured without modifying the existing HBT technology, such as masks or additional processing steps. Only the structure's layout geometries are adjusted to create an optical window opening. This strategy guarantees low cost and simple compatibility with SiGe circuits on the same chip, enabling the direct integration of SiGe HPTs into an industrial foundry [Figure 1](#).

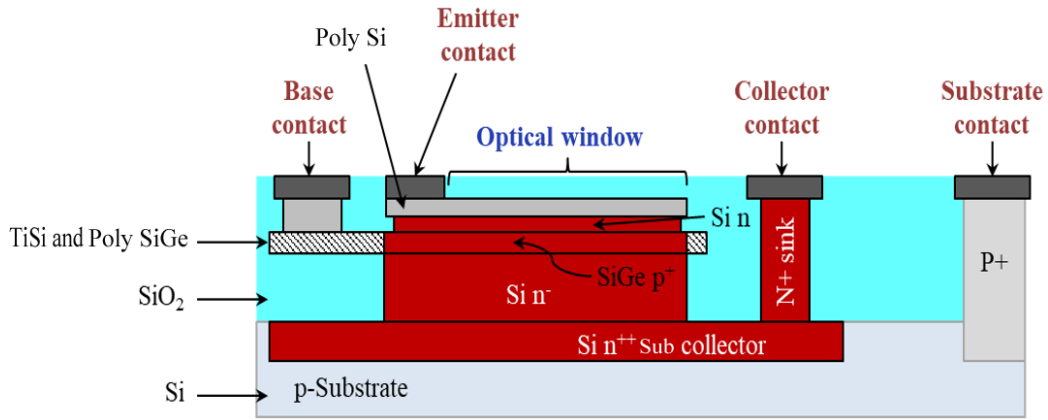


**Figure 1.** Shows the structure of the considered SiGe HPT Telefunken GmbH 80-GHz.

To gain a better understanding of the SiGe HPT, we analyzed its equivalent electrical schemas, as shown in Figure 2 [22]. The electrical schema of the HPT is a crucial element in its performance, consisting of the active and extended areas, both of which are based on the Ebers & Moll model. The active area is responsible for amplifying the signal, while the extended area is responsible for collecting the signal. The model incorporates accurately modeled non-ideal diodes, resistors, and capacitors using ADS. The mathematical equations defined by the Ebers & Moll model are employed to precisely capture the behavior of these components.

Additionally, block modeling involves subtracting and incorporating two capacitances to enable the HPT to operate at multiple bias points. Overall, the electrical model of the HPT consists of two corresponding phototransistors that form the active and extended areas. By accurately modeling these areas and their respective components, it is possible to optimize the performance of the HPT and improve its effectiveness in modern communication systems. We evaluate the performance of this electrical model by studying various validation options for the HPT’s electrical model in the nonlinear domain and examining its noise characteristics.

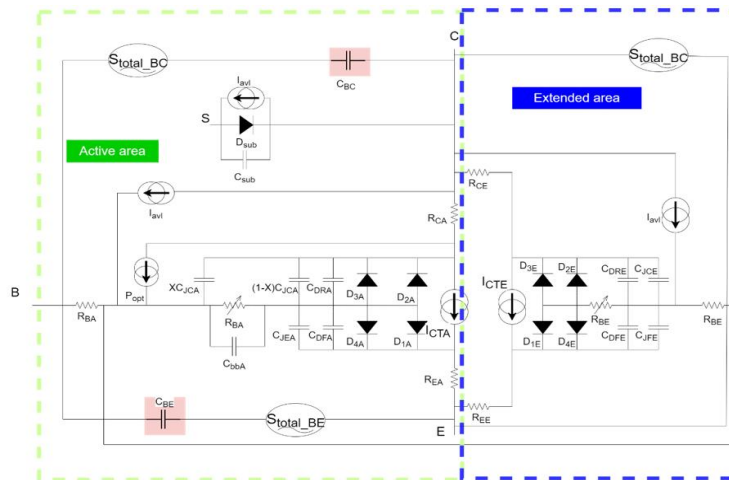


**Figure 2.** Electrical schemas of the considered SiGe HPT 10SQxEBC.

The main performance parameters of SiGe/Si HPT devices are the error vector magnitude (EVM), third-order intercept point (IP3), and noise characteristics. These parameters are of particular importance, and we conduct a comprehensive analysis to gain an understanding of the functioning of SiGe/Si HPT devices and identify avenues for their improvement in high-speed optical communication systems. Additionally, we examine how different design and fabrication methods affect the performance of these devices and provide suggestions for future research in this area.

This paper aims to give a detailed analysis of the essential performance metrics of SiGe/Si HPT devices, with the goal to assist in designing high-speed optical communication systems that can effectively harness the advanced capabilities offered by these devices. The performance analysis is based on precise measurements of EVM, IP3, and noise characteristics.

### 3. Performance for Application LTE Simulate EVM

In this section, we delve deeper into the concept of Error Vector Magnitude (EVM) and its measurement in the context of an LTE device. EVM is a critical performance metric that characterizes the signal quality generated by a communication system. It measures the deviation of the received signal from the ideal signal that would be expected if no noise or distortion were present. EVM is commonly used to characterize high-speed optical communication systems, such as phototransistor HPTs.

To measure EVM, vector signal analyzers (VSAs), real-time analyzers, or other instruments that capture a time record and perform a Fast Fourier Transform (FFT) for frequency domain analysis are used. Prior to EVM calculations, the signals are downconverted to ensure that the signal is within a frequency range that the instrument can analyze. According to the LTE standard, the behavior of Error Vector Magnitude (EVM) is typically below the 64-QAM requirements [26], with an EVM threshold of less than 8% [13].

Normalization is an essential step in EVM calculations. Different modulation systems, such as BPSK, 4-QAM, 16-QAM, etc., have different amplitude levels. Normalization is typically performed to calculate and compare EVM measurements effectively [27]. The normalization is derived so that the mean square amplitude of all possible symbols in the constellation of any modulation scheme is equal to one. This allows for the equal comparison of EVM values for different modulation schemes. EVM is computed as the root-mean-square (RMS) value of the difference between a set of measured and ideal symbols. These differences are averaged over multiple symbols and are often expressed as a percentage of the average power per symbol of the constellation. Therefore, EVM can be mathematically expressed as Arshad, et al. [28].

$$EVM = \frac{1}{M} * \sqrt{\frac{\sum_{n=1}^N |R_{x,n} - T_{x,n}|^2}{\sum_{n=1}^N |T_{x,n}|^2}} \quad (1)$$

Where:

M is the total number of symbols.

$T_{x,n}$  the ideal signal.

$R_{x,n}$  the received signal.

EVM is a crucial parameter in evaluating the quality of communication systems. It measures the deviation of the received signal from the ideal signal that would be expected if no noise or distortion were present. Normalization is a critical step in EVM calculations, and it is derived in such a way that the mean square amplitude of all possible symbols in the constellation of any modulation schemes is equal to one.

To generate the LTE signal, a 10 ms signal frame with a passband frequency of 750 MHz was created. This signal was then transmitted to the SiGe HPT, which efficiently detected and amplified the weak optical signals. To further the signal strength, a 40 dB Gain Low Noise Amplifier (LNA) was used to amplify the HPT output. The amplified signal was then fed into a Vectorial Signal Analyzer, which downconverter the passband signal to the baseband for EVM computation.

Figure 3 displays the EVM of PTH simulation obtained by modulating a signal using 16-Quadrature Amplitude Modulation. This modulation scheme is commonly employed in communication systems to transmit data through radio waves, enabling the transmission of four bits of data per symbol. It modulates the amplitude and phase of the carrier signal to represent the data.

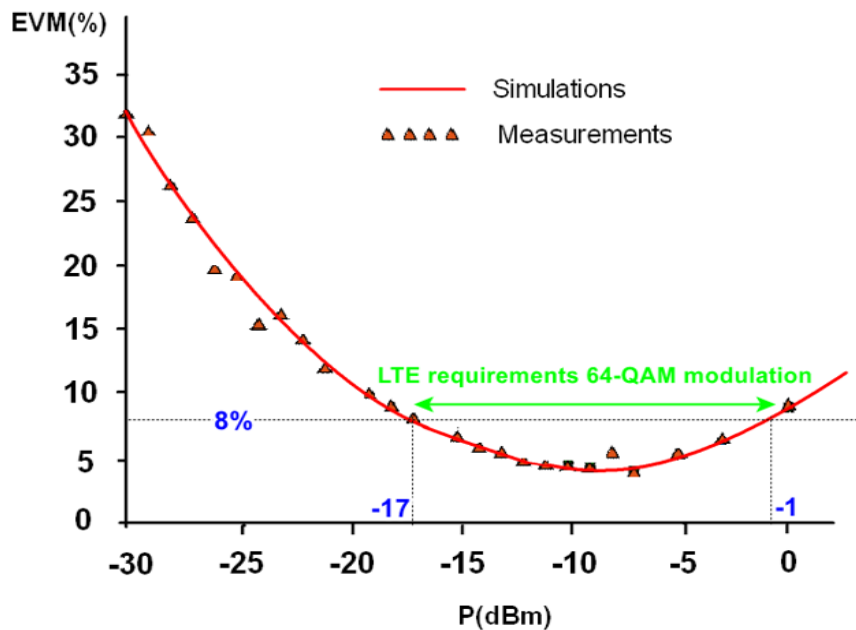


Figure 3. EVM simulation and measures for SiGe HPT 10SQxEBC showed power dBm could use for LTE.

Figure 3 presents a comparison between the simulation results and the measurements obtained from the LTE setup using the phototransistor 10SQxEBC for EVM quantification. The simulations were conducted by injecting a vector signal generator over fiber, which is an electrical device that produces direct current (DC) electricity.

As can be seen in the figure, there is good agreement between the measurements and the simulations performed to determine the EVM. Additionally, Figure 2 illustrates that the EVM value remains below 8% when using the HPT, which meets the requirements of the LTE standard for 64-QAM modulation [29] within the input power range of -17 dBm to -1

dBm. Therefore, our HPT model can be used for an LTE link in modulation. These results validate the accuracy and reliability of our simulation approach and affirm the suitability of the HPT for integration into LTE systems.

**4. Evaluation of IP3 on HPT**

Microwave fiber-optic links that operate at high-performance levels require precise and reliable system components to ensure optimal performance. Among these components, high-frequency optical detectors are particularly crucial as they significantly determine the overall system performance. It explains the nonlinear distortions that can occur in HPT at high incident optical powers and higher frequencies, and their potential impact on link performance. The absence of precise requirements for HPT linearity based on link performance is highlighted. To address this gap, the paper introduces proposed performance criteria and presents measurements of detectors designed to meet these criteria.

Despite extensive research on this topic, there has been a lack of clear performance requirements for photodetector linearity based on link performance. Some authors in the literature have managed to define values for IP3 [30]. The modulator's input third-order intercept point (IP3) can be calculated through analytical methods, as described in reference [31] for considering IP3, including only by modulation.

$$IP3 = 4I_{ph}^2 R_L \quad (2)$$

Where:

$I_{ph}$ : Photocurrent of HPT.

$R_L$ : Load resistance of HPT.

For the spurious-free dynamic range (SFDR), when we include nonlinearities of HPT the degradation in the link can illustrate by Equation 3 [30]:

$$\Delta SFDR = \left(\frac{2}{3}\right) 10 \log \left[ 1 + 10^{\frac{-\Delta IP3}{10}} \right] \quad (3)$$

Where:

$\Delta IP3$ : The difference between IP3 of HPT and modulator-limited link.

$\Delta SFDR$ : Difference in the modulator limited SFDR.

The SFDR of the link.

The HPT 10SQxEBC was developed to deliver IP3 requirements for fiber optic links and was included in bloc detection [30].

Figure 4 plots the RF output power from the HPT as a function of the incident optical modulation power. The incident optimal modulation power is determined by multiplying the optical power by the optical modulation index. The IP3, referenced to the RF output power of HPT, is also shown in the plot. In our experiment, we applied a bias current of 2.3 mA, with a bias voltage of  $V_{BC} = 0.89$  V and  $V_{CE} = 2$  V. The third-order intermodulation product can be found at frequencies of 2.39 GHz and 2.42 GHz, along with the two converted RF test frequencies at 2.40 GHz and 2.41 GHz.

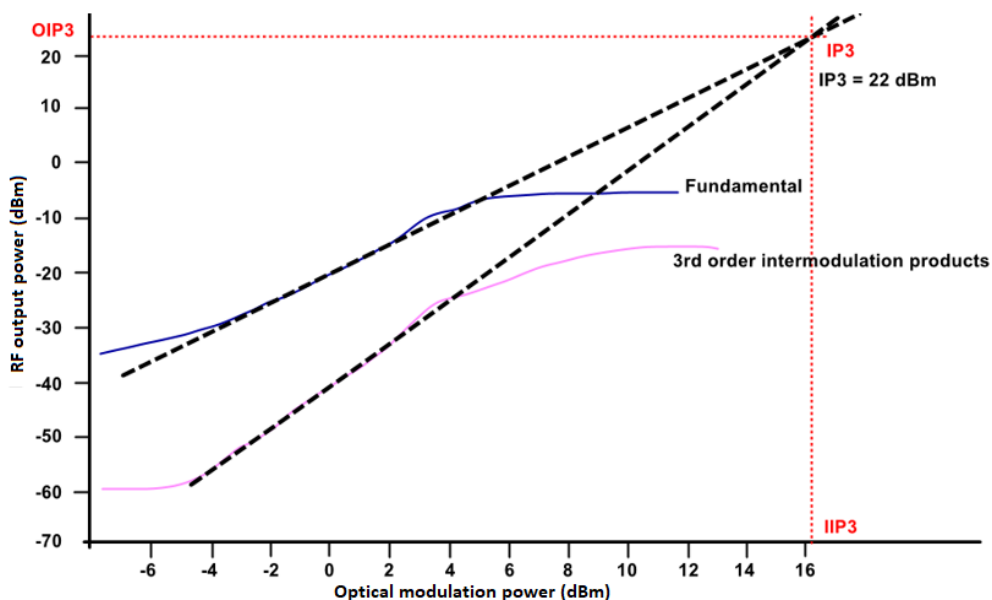


**Figure 4.** Simulation intermodulation of harmonic balance showing IP3 of 22 dBm at a center frequency 2.4 GHz with 2.3 mA.

The results of our study on the high-power transistor (HPT) 10SQxEBC indicate that the IP3 value obtained at operating conditions of 2.4 GHz frequency and 2.3 mA photocurrent is 22 dBm. This value corresponds to the IP3 accuracy range of +/- 1 dBm, as reported in the literature. Therefore, we conclude that the HPT is suitable for use in optical links. These findings

have significant implications for designing and developing high-power transistors for future optical communication systems. Our study highlights the importance of accurate IP3 measurements and their role in ensuring the reliability and efficiency of optical communication systems.

### 5. Evaluation of Noise on HPT

The HPT model has been completed by studying the nonlinearities and defining a noise model that quantifies the influence of noise on the developed HPT model. In recent years, there has been a growing interest in the study of low-level electrical signals, particularly in applications requiring high accuracy and precision, such as in medical and scientific research. Accurate measurement of electrical signals is crucial in these fields to obtain meaningful results.

However, electrical signals can be affected by various types of noise, including pulse transient. This type of noise results from the interaction between the measurement system and the signal being measured, and it can significantly impact the accuracy of the measurements. To address this issue, the HPT noise model was developed to quantify and correct for pulse-transient and noise. The model considers the effects of several key parameters, including the pulse amplitude, and duration, signal path impedance, and the frequency response of the measurement system.

The development of the HPT noise model has resulted in significant improvements in the accuracy of electrical signal measurements. By incorporating the model into measurement systems, researchers and engineers can have confidence in the accuracy and reliability of their results.

However, it is essential to note that the HPT noise model may not be applicable to all electrical signals and measurement systems. In some cases, alternative noise models or measurement techniques may be more appropriate. Nevertheless, the HPT noise model remains a valuable tool for many applications, and its usage is expected to continue growing in the coming years.

There has been a growing interest in the study of low-level electrical signals, particularly in applications where accurate measurement is crucial for obtaining meaningful results. However, electrical signals can be affected by various types of noise. In the context of semiconductors, there are primarily five types of noise: thermal noise or the Johnson effect in ohmic regions, which is associated with the thermal agitation of electrons; shot noise or grain noise, generated when electrons cross a potential barrier, resulting in popcorn noise caused by unoccupied space in the crystallographic network of HPT SiGe; Flicker noise, or 1/f noise, generally caused by surface recombination due to the crystallographic network of HPT; and avalanche noise, which is not included in our model because the operating points are below the avalanche region. The HPT 10SQxEBC noise model has been carefully developed to account for the impact of these different noises in SiGe semiconductors.

The thermal noise, generated by the thermal agitation of the charge carriers, has been incorporated into the model through a simplification of the equation provided by Nyquist [32]:

$$S_{thermal} = 4 \left[ \frac{hf}{2} + \frac{hf}{e^{hf/kT} - 1} \right] R \quad (4)$$

Where:

HF: Electromagnetic energy.

K: Boltzmann constant.

T: Temperature at Kelvin.

H: Planck constant.

R: pure resistance of noise.

In practice (ambient temperature), the equation simplifies if we consider that  $hf \ll kT$ .

$$S_{thermal-n} = 4kTR \quad (5)$$

The shot noise generated by the movement of charge carriers in junctions to cross the potential barrier is given by Kramers [33] in the form.

$$\overline{i_{th}^2} = 2qI\Delta f \quad (6)$$

Where:

q: The charge of the electron.

I: The direct current flowing through the junction.

Δf: Frequency band.

For shot noise Power Spectral Density (PSD) depends only on the current, so after deriving  $i_{th}$  we have:

$$S_{shot-n} = 2qI \quad (7)$$

Equation 7 represents the shot noise power spectral density in a circuit where q is the charge of the electron and I is DC (direct current) bias current flowing through the circuit.

Generation-recombination noise results from unoccupied spaces in the crystal lattice and depends on temperature and polarization conditions. It is referred to as popcorn noise [34] and the following equation is used for modeling purposes.

$$S_{G-R}(f) = K_B \frac{I^{AB}}{1 + (\frac{f}{FB})^2} \quad (8)$$

Where  $K_B$ , AB and FB are model parameters that describe the behavior of the system's noise power spectral density. AB describes how the noise power depends on the current, while FB determines the range of frequencies over which the noise power is significant. AB is the exponent of the current I in the numerator of the equation. It is often referred to as the "excess noise factor" and characterizes the relationship between the noise power and the current. When AB=1, the noise power is

directly proportional to the current, known as "white" or "shot" noise. When  $AB > 1$ , the noise power is considered "excess" and increases faster than the current. Conversely, when  $AB < 1$ , the noise power decreases as the current increases.

FB represents the frequency at which the noise power spectral density is half of its value at DC (zero frequency). It is often called the "bandwidth" of the system and indicates the range of frequencies where the noise power is significant. The denominator of the equation represents a low-pass filter with a corner frequency of FB, which attenuates the noise power at high frequencies. Therefore, FB determines the high-frequency roll-off of the noise power spectral density.

Flicker noise arises from the presence of a constant base current and is used to assess the stability of applications. Several expressions have been proposed to quantify the flicker noise, with the model proposed by Hooge providing the best representation of this type of noise in the HPT 10SQxEBC model we have developed. It can be expressed using the following function [35].

$$S_{1/f}(f) = \frac{\alpha_H I_B^\alpha}{f^{\gamma.N}} \quad (9)$$

Where:

$\alpha_H$  is Hooge constant.

$\alpha$  and  $\gamma$  are material constants.

$N$  is the number of charge carriers in the region where the noise is generated.

Avalanche noise appears for very high reverse junction voltages leading to a collision of charge carriers with the crystallographic network. The PSD can be expressed as.

$$S_{A-n} = 2MqI \quad (10)$$

Where  $M$  is the multiplicative factor that characterizes an avalanche.

Studies on the HPT 10SQxEBC have indicated that avalanche noise becomes apparent beyond 4V [25]. However, in our case, we focus on analyzing the noise at valid polarization points within the model, ensuring that the voltage remains below the avalanche voltage. This allows us to eliminate the influence of avalanche noise from our study. In our model, we incorporated various types of noise mentioned below to examine their impact on the output signal.

Furthermore, in the noise study system we have developed, we can consider the base current and collector current as independent variables, allowing us to treat the noises as non-interdependent [36].

The total noise power spectral density can be interpreted as follows:

$$S_{total} = 4kTR + 2qI + K_B \frac{I^{AB}}{1 + (\frac{f}{FB})^2} + \frac{\alpha_H I_B^\alpha}{f^{\gamma.N}} \quad (11)$$

Since the noises in the HPT 10SQxEBC have all appropriately been defined, the next step is to locate the noise sources on the phototransistor and incorporate them into the established model. In common-emitter configurations, thermal and shot noise primarily originate from the base-emitter (BE) and emitter-collector (EC) junctions. On the other hand, flicker noise is associated with the collector region, where a continuous current flows through the HPT. The noise phenomenon is linked to the current flowing through the device, as illustrated in Figure 5. The mathematical formulation enables us to determine the power spectral density of a random noise current source. It is important to note that bipolar transistors inherently amplify current.

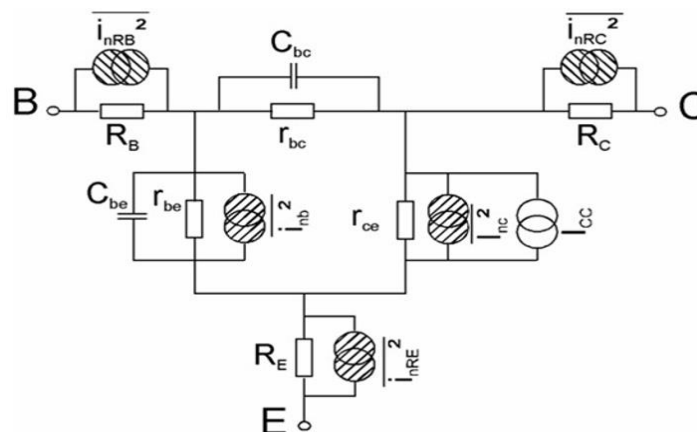
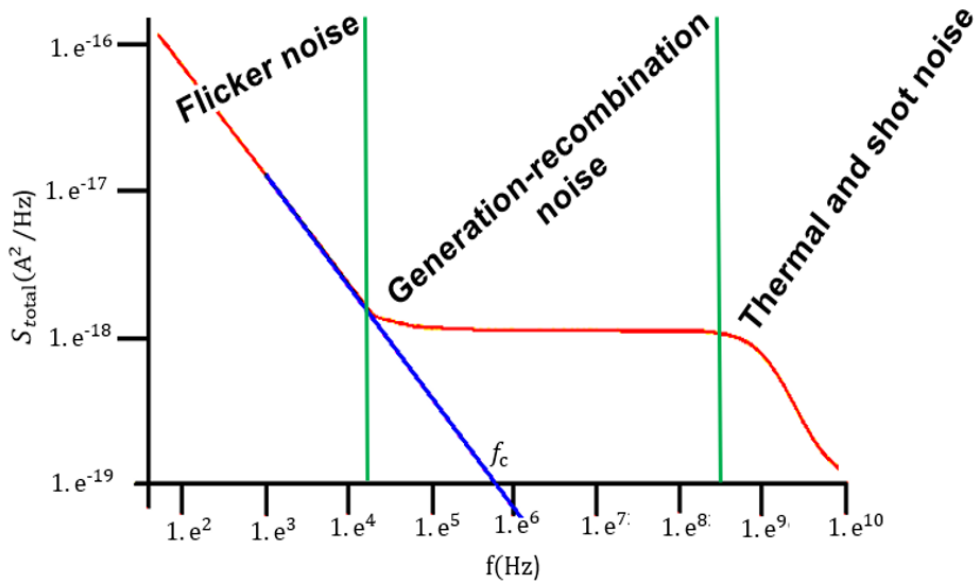


Figure 5. Equivalent Circuit of an HPT 10SQxEBC showing noises sources.

We present the electrical equivalent circuit of HPT noise in Figure 5. The developed model examines the main noise sources in a transistor, such as thermal, flicker generation-recombination, and shot noise. Figure 5 illustrates the association of physical resistors  $R_B$ ,  $R_C$ ,  $R_E$  with the thermal noise source introduced by Equation 6 for each resistor. Our developed model considers the collector and base currents as independent variables [25]. As a result, we have a separate shot noise

contribution from the base that is not dependent on the collector's shot noise, as shown in Equation 8. In Figure 5, we have dissociated the two types of noise to provide a clear illustration of their individual contributions.

Once the noise source locations have been determined, we proceed to simulate Figure 5 to obtain Figure 6.



**Figure 6.** Simulation results of the output HPT noise spectral density over a wide frequency range.

Figure 6 illustrates the impact of various noise sources in the developed HPT, which was optimized by adjusting the noise model parameters based on literature under the same conditions and bias point. The frequency range of interest was within the HPT's corner frequency  $f_c$  (10Hz-10kHz). The noise figure in Figure 6 displays the influence of each noise source. We applied a log-on Equation 11 to determine the model parameters and extracted the values at different frequencies. The extracted parameters of all noise sources used for characterizing the HPT noise are presented in Table 1. These results provide a comprehensive understanding of the noise performance of the HPT and demonstrate its suitability for use in optical links. Moreover, they can be used to improve the overall design and performance of similar devices in the future.

**Table 1.** Model parameters of the noise model of the 10SQxEBC HPT.

Junctions	Base-emitter		Base-collector	
	Parameters	Value	Parameters	Value
<b>Noises types</b>				
Generation-recombination noise	$K_B$	$6.5 e^{-11}$	$K_C$	$1.95 e^{-5}$
	AB	1.18	AB	1.8
	FB	2.75	FB	2.44
Flicker noise	$\alpha$	1.5	$\alpha$	1.3
	$\gamma$	1	$\gamma$	1
Shot noise	S(pV)	47.62	S(pV)	281.6

### 6. Conclusion

The studies conducted on our SiGe/Si heterojunction bipolar phototransistor HPT model have revealed its great potential for high-speed optical communication systems. In particular, the research has focused on the device's nonlinear behavior, EVM, IP3, and noise performance, while also optimizing its high-frequency response and exploring new applications. Researchers continue to study and improve upon these devices, exploring ways to further enhance their performance for high-speed optical communication systems. The results presented in this paper showcase the successful development and optimization of the noise model for the HPT, which in turn offers valuable insights into its noise performance under various operating conditions. The quality of our developed model has been evaluated through rigorous testing and simulation, instilling a high degree of confidence in its accuracy.

Furthermore, the study of nonlinearities in the HPT has provided valuable information about its behavior in the presence of high-frequency signals, which is crucial for designing and optimizing high-speed optical communication systems. This research has contributed to the growing body of knowledge surrounding the use of SiGe/Si HPT devices in high-performance optical communication systems. Overall, the potential of SiGe/Si HPT devices for high-speed optical communication systems is evident. The results presented here serve as a foundation for further research and development of these devices, driving advancement in faster, more reliable, and more efficient high-speed optical communication systems.

## References

- [1] M. N. Abedin, M. R. Islam, S. H. Khan, M. S. Islam, and M. Z. Kabir, "Design and analysis of a SiGe/Si HBT-based phototransistor for high-speed optical communication systems," *Optik - International Journal for Light and Electron Optics*, vol. 163, pp. 207-214, 2018.
- [2] A. M. Alzaher, M. F. Alhareb, R. A. Abd-Alhameed, A. J. Salim, and J. M. Noras, "Nonlinear behavior analysis of SiGe HPT device for high-speed optical receivers," presented at the Progress in Electromagnetics Research Symposium - Spring (PIERS), 2019.
- [3] M. Ma, L. Zhang, Z. Chen, Q. Zhang, and L. Liu, "Investigation of EVM enhancement in SiGe HBT based phototransistor," *Optik - International Journal for Light and Electron Optics*, vol. 181, pp. 195-201, 2019 .
- [4] H. J. Schenk and H. Zimmermann, "SiGe heterojunction bipolar transistors for high-speed optoelectronics," *IEEE Journal of Selected Topics in Quantum Electronics*, vol. 1, no. 3, pp. 859-868, 1995.
- [5] R. A. M. Khan, H. P. Laba, and M. H. Bin Baharudin, "Pre-distortion for third order intermodulation suppression in SiGe HBT-based phototransistors for high-speed optical communication,," *International Journal of Applied Engineering Research*, vol. 12, no. 18, pp. 7976-7980, 2017.
- [6] S. H. Jeon, H. J. Shin, and J. H. Kim, "Digital predistortion techniques for intermodulation distortion suppression in SiGe HBT-based photoreceivers," *IEEE Transactions on Microwave Theory and Techniques*, vol. 58, no. 4, pp. 928-937, 2010.
- [7] C. K. Sun, K. H. Chien, and C. W. Chiu, "Noise characteristics of Si/SiGe heterojunction bipolar phototransistors for high-speed optical communications," *IEEE Journal of Quantum Electronics*, vol. 46, no. 6, pp. 871-879, 2010.
- [8] J. Kim, J. Heo, and J. Kim, "Optical signal to noise ratio enhancement using a SiGe HBT-based photoreceiver with 1st- and 2nd-order high-pass active filters," *Sensors*, vol. 19, no. 18, pp. 3869-3878, 2019
- [9] H. Xiong, X. Zhang, and Y. Fu, "A novel method for suppressing noise in SiGe HBT-based optoelectronic devices," *IEEE Photonics Technology Letters*, vol. 22, no. 24, pp. 1823-1825, 2010.
- [10] F. Ouyang, Z. Zhang, L. Wang, Y. Liu, and Z. Han, "Design of SiGe HBT-based phototransistors with improved high-frequency performance," *IEEE Photonics Journal*, vol. 10, no. 6, pp. 1-11, 2018.
- [11] V. Giordano and R. De Rose, "SiGe/Si heterojunction bipolar phototransistors: New perspectives for sensing applications," *Sensors and Actuators A: Physical*, vol. 122, no. 1, pp. 15-23, 2005.
- [12] J. Zhang, X. Zhang, Q. Huang, and X. Meng, "Characterization of a SiGe/Si HPT detector for X-ray imaging applications, nuclear instruments and methods in physics research section A: Accelerators, spectrometers," *Detectors and Associated Equipment*, vol. 958, p. 162547, 2020.
- [13] G. Gu, F. Qin, J. Zhang, X. Xie, and S. Li, "SiGe/Si HPT optoelectronic devices based on molecular beam epitaxy," *Journal of Semiconductors*, vol. 37, no. 1, p. 014008, 2016.
- [14] R. N. Nottenburg, G. Livescu, and R. T. Young, "GaAs and InP bipolar transistors with SiGe layers for heterojunction bipolar transistors," *Journal of Applied Physics*, vol. 76, no. 8, pp. 4621-4632, 1994.
- [15] R. T. Young, G. Livescu, R. N. Nottenburg, and M. R. Melloch, "High-performance InP/InGaAs heterojunction bipolar transistors grown by metal-organic chemical vapor deposition," *IEEE Electron Device Letters*, vol. 16, no. 3, pp. 98-100, 1995.
- [16] Y. Wei, L. Gu, Y. Zhang, Y. Cheng, L. Liu, and L. Wang, "Characterization and modeling of heterojunction phototransistor for high-speed optical communication systems," *Optik*, vol. 156, pp. 515-520, 2018.
- [17] R. Zhang, Y. Chen, Z. Zhou, L. Li, J. Yuan, and K. Li, "Design and fabrication of high-speed Si/SiGe heterojunction phototransistors," *Journal of Semiconductors*, vol. 41, pp. 1-6, 2020.
- [18] M. Chen, Q. Zhang, Y. Li, S. Chen, and C. Liu, "Radio-over-fiber-based wireless sensor networks," in *Proceedings of the 2017 International Conference on Wireless Networks and Mobile Communications (ACM, 2017)*, 2017, pp. 40-45.
- [19] A. Rangarajan, "Silicon-germanium heterojunction phototransistor for high-speed data communication," *Journal of Optoelectronics and Advanced Materials*, vol. 19, no. 3-4, pp. 227-234, 2017.
- [20] N. Gupta, "A review of silicon-germanium heterojunction bipolar transistors," *International Journal of Scientific and Research Publications*, vol. 3, no. 5, pp. 1-6, 2013.
- [21] S. K. Bose, A. R. M. Alamoud, and M. A. Hasan, "High-speed optical communication systems using SiGe/Si HPT devices," *Journal of Optoelectronics and Advanced Materials*, vol. 22, no. 1-2, pp. 15-27, 2020.
- [22] A. Bennour, Z. Tegegne, S. Mazer, J. Polleux, M. El Bekkali, and C. Algani, "Large-signal static compact circuit model of siGe heterojunction bipolar phototransistors: Effect of the distributed nature of currents," *IEEE Transactions on Electron Devices*, vol. 65, no. 3, pp. 1029-1035, 2018. <https://doi.org/10.1109/ted.2017.2788447>
- [23] R. Plana *et al.*, "Low-frequency noise in millimeter-wave Si/SiGe heterojunction bipolar transistors," in *Proceedings of 1995 IEEE MTT-S International Microwave Symposium, Orlando, FL, USA*, 1995, vol. 3, pp. 1431-1434.
- [24] M. D. Rosales, J. L. Polleux, and C. Algani, "Design and implementation of SiGe HPTs using an 80GHz SiGe bipolar process technology," presented at the 8th IEEE International Conference on Group IV Photonics, London, 2011.
- [25] G. Liu, A. Ç. Ulusoy, A. Trasser, and H. Schumacher, "64 to 86 GHz VCO utilizing push-push frequency doubling in a 80 GHz ft SiGe HBT technology," presented at the 2010 Topical Meeting on Silicon Monolithic Integrated Circuits in RF Systems (SiRF), New Orleans, LA, USA, 2010.
- [26] 3GPP. (2017). LTE evolved universal terrestrial radio access (E-UTRA); base station (BS) radio transmission and reception (Release 14.3). Technical Specification 36.101. Retrieved from [https://www.3gpp.org/ftp/Specs/archive/36\\_series/36.101](https://www.3gpp.org/ftp/Specs/archive/36_series/36.101)
- [27] A. K. Wang, R. Liganowski, J. Castro, and A. Mazzara, "EVM simulation and analysis techniques," presented at the MILCOM 2006 - 2006 IEEE Military Communications Conference, Washington, DC, USA, 2006.
- [28] K. Arshad, K. Nisar, M. Azam, and S. Rehman, "A comparative study on the performance of digital communication systems using different modulation techniques," *2016 Journal of Electronics and Communication Engineering*, vol. 11, pp. 17-22, 2016.
- [29] J. Nanni, Z. G. Tegegne, C. Algani, G. Tartarini, and J.-L. Polleux, "Use of SiGe photo-transistor in RoF links based on VCSEL and standard single mode fiber for low cost LTE applications," in *2018 International Topical Meeting on Microwave Photonics (MWP)*, 2018: IEEE, pp. 1-4.
- [30] D. Scott *et al.*, "Measurement of IP3 in pin photodetectors and proposed performance requirements for RF fiber-optic links," *IEEE Photonics Technology Letters*, vol. 12, no. 4, pp. 422-424, 2000. <https://doi.org/10.1109/68.839039>
- [31] L. J. Lembo *et al.*, "Optical electroabsorption modulators for wideband, linear, low-insertion-loss photonic links," in *Photonic Device Engineering for Dual-Use Applications*, 1995, vol. 2481: SPIE, pp. 185-196.

- [32] H. Nyquist, "Thermal agitation of electric charge in conductors," *Physical Review*, vol. 32, no. 1, pp. 110-113, 1928. <https://doi.org/10.1103/physrev.32.110>
- [33] H. A. Kramers, "On the theory of statistical radiation," *Proceedings of the Royal Academy of Sciences of the Netherlands*, vol. 26, no. 7, pp. 779-787, 1924.
- [34] G. Massobrio and P. Antognietti, *Semiconductor device modeling with SPICE*. New York: Mc Graw- Hill, 1993.
- [35] F. N. Hooge, "1/f noise is no surface effect," *Physics Letters A*, vol. 29, no. 3, pp. 139-140, 1969.
- [36] P. Sakalas, M. Schroter, and H. Zirath, "Mm-Wave noise modeling in advanced SiGe and InP HBTs," *Journal of Computational Electronics*, vol. 14, no. 1, pp. 62-71, 2015. <https://doi.org/10.1007/s10825-015-0664-6>